Supplementary Information for:

Programmable lithium niobate photonic chip for near-ideal path entanglement and frequency entanglement

J.C. Duan et al.

*Corresponding author. Email: pingxu520@nju.edu.cn

Note 1: Derivation of on-chip BRHOM interference on MZI

The transfer matrix of MZI can be expressed as

$$\begin{pmatrix} \sqrt{t_0}e^{iA} & \sqrt{r_0}e^{iB} \\ \sqrt{r_0}e^{iB} & \sqrt{t_0}e^{-iA} \end{pmatrix}, \tag{1}$$

where

$$\sqrt{r_0} = \left| 2\sqrt{r}\sqrt{t}\cos\left(\frac{\varphi_c}{2}\right) \right|, \quad \sqrt{t_0} = \sqrt{1-4tr\cos^2\left(\frac{\varphi_c}{2}\right)}, \tag{2}$$

$$e^{iB} = \frac{i\cos\left(\frac{\varphi_c}{2}\right)}{\left|\cos\left(\frac{\varphi_c}{2}\right)\right|}, \quad e^{iA} = \frac{i\sin\left(\frac{\varphi_c}{2}\right)+\cos\left(\frac{\varphi_c}{2}\right)(2t-1)}{\sqrt{1-4tr\cos^2\left(\frac{\varphi_c}{2}\right)}}, \quad e^{-iA} = \frac{-i\sin\left(\frac{\varphi_c}{2}\right)+\cos\left(\frac{\varphi_c}{2}\right)(2t-1)}{\sqrt{1-4tr\cos^2\left(\frac{\varphi_c}{2}\right)}}. \tag{3}$$

Obviously, the phase relationship $A+(-A)+2B=\pm\pi$. If $r_0=\frac{1}{2}$, there will be $\cos(\varphi_c)=\frac{1}{4t(1-t)}-1$

and $A_0=\arccos(\frac{2t-1}{2\sqrt{t}\sqrt{1-t}})$. The normalized coincidence rates are

$$R_{|2,0\rangle} = \left|\left\langle \Psi_{|2,0\rangle} \middle| \Psi_0 \right\rangle\right|^2 = \frac{1}{\left(1+|m|^2\right)}\left(r_0^2+m^2t_0^2-2mr_0t_0\cos\left(\varphi_s-2A\right)\right) \tag{4}$$

$$R_{|0,2\rangle} = \left|\left\langle \Psi_{|0,2\rangle} \middle| \Psi_0 \right\rangle\right|^2 = \frac{1}{\left(1+|m|^2\right)}\left(m^2r_0^2+t_0^2-2mr_0t_0\cos\left(\varphi_s-2A\right)\right) \tag{5}$$

$$R_{|1,1\rangle} = \left|\left\langle \Psi_{|1,1\rangle} \middle| \Psi_0 \right\rangle\right|^2 = \frac{2}{\left(1+|m|^2\right)}r_0t_0\left(1+m^2+2m\cos\left(\varphi_s-2A\right)\right) \tag{6}$$

Note 2: Derivation the visibilities of on-chip BRHOM and off-chip HOM interference

The imperfect BRHOM interference reduces the quality of output photons. The visibility of on-chip BRHOM and off-chip HOM interference can be evaluated by two empirical formulas:

$$V_{BRHOMI} \equiv \frac{R_{\max}-R_{\min}}{R_{\max}+R_{\min}}, \tag{7}$$

$$V_{HOMI} \equiv \frac{R_{\max}-R_{\min}}{R_{\max}}. \tag{8}$$

It is assumed that the spectrum of photons is identical. Though the output photon pairs are set in the antibunching state, some remaining bunching photons are still on the R_1 and R_2 paths due to incomplete BRHOM interference. The remaining bunching photons will also have phase-sensitive interference in off-chip HOM interference, which will reduce its visibilities and, consequently, degrade the quality of the resources. Based on Eq. (7) and (8), the extreme values of curves can be calculated by

$$R_{|2,0\rangle}^{\max}=\frac{\left(r_0+mt_0\right)^2}{\left(1+|m|^2\right)},\quad R_{|0,2\rangle}^{\max}=\frac{\left(mr_0+t_0\right)^2}{\left(1+|m|^2\right)},\quad R_{|1,1\rangle}^{\max}=\frac{2r_0t_0\left(1+m\right)^2}{\left(1+|m|^2\right)},\tag{9}$$

$$R_{|2,0\rangle}^{\min}=\frac{\left(r_0-mt_0\right)^2}{\left(1+|m|^2\right)},\quad R_{|0,2\rangle}^{\min}=\frac{\left(mr_0-t_0\right)^2}{\left(1+|m|^2\right)},\quad R_{|1,1\rangle}^{\min}=\frac{2r_0t_0\left(1-m\right)^2}{\left(1+|m|^2\right)}.\tag{10}$$

The visibility of BRHOM is

$$V_{\mathrm{BRHOMI}(|1,1\rangle)}=\frac{2m}{1+m^2},\quad V_{\mathrm{BRHOMI}(|2,0\rangle)}=\frac{2mr_0t_0}{m^2t_0^2+r_0^2},\quad V_{\mathrm{BRHOMI}(|0,2\rangle)}=\frac{2mr_0t_0}{m^2r_0^2+t_0^2}.\tag{11}$$

Meanwhile, the visibility of the off-chip HOM interference is related to the residual bunching photons of the on-chip BRHOM interference. Out of the coherence time, the photon pairs do not interfere and the coincidence counts are maximal

$$R_{\mathrm{HOMI}}^{\max}=\frac{1}{2}\times\frac{2r_0t_0\left(1+m\right)^2}{\left(1+|m|^2\right)}+\frac{1}{2}\times\frac{\left(r_0-mt_0\right)^2}{\left(1+|m|^2\right)}+\frac{1}{2}\times\frac{\left(mr_0-t_0\right)^2}{\left(1+|m|^2\right)}=\frac{1}{2}.\tag{12}$$

The first (second and third) part on the right is the effective coincidence of the contribution of antibunching (bunching) photons. When the time delay is zero, the antibunching photons fully interfere and contribute no counts, while bunching photons transform to coincidence counts, as described by

$$R_{\mathrm{HOMI}}^{\min}=\frac{\left(\sqrt{R_{|0,2\rangle}^{\min}}+\sqrt{R_{|2,0\rangle}^{\min}}\right)^2}{2}.\tag{13}$$

The visibility of HOM is

$$V_{\mathrm{HOMI}}=1-\left(\sqrt{R_{|0,2\rangle}^{\min}}+\sqrt{R_{|2,0\rangle}^{\min}}\right)^2$$

Through the computation from Eq. S(7)-S(13), substituting $t_0=r_0=1/2$, the visibilities are

$$V_{\mathrm{BRHOMI}(|1,1\rangle)}=V_{\mathrm{BRHOMI}(|2,0\rangle)}=V_{\mathrm{BRHOMI}(|0,2\rangle)}=V_{\mathrm{HOMI}}=\frac{2m}{1+m^2}.\tag{14}$$

The theoretical visibilities of BRHOM and HOM interference are equal. Mapping the Eq. S(8) as follows

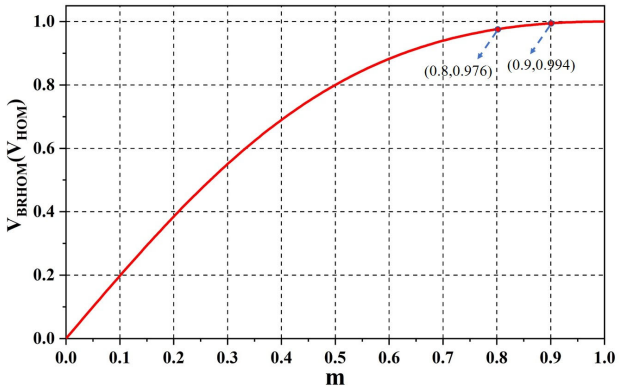

Fig.S1 Theoretical Visibility of BRHOM and HOM interference varies with *m*. When the *m* is approaches 1, the change of visibility is insensitive.

Note 3: BRHOM interference for degenerate and nondegenerate photons

The main text has given representative BRHOM interferences of a pair of photons with 1565 nm and with a separation of 40 nm. In this part, we will give the remaining interference fringes.

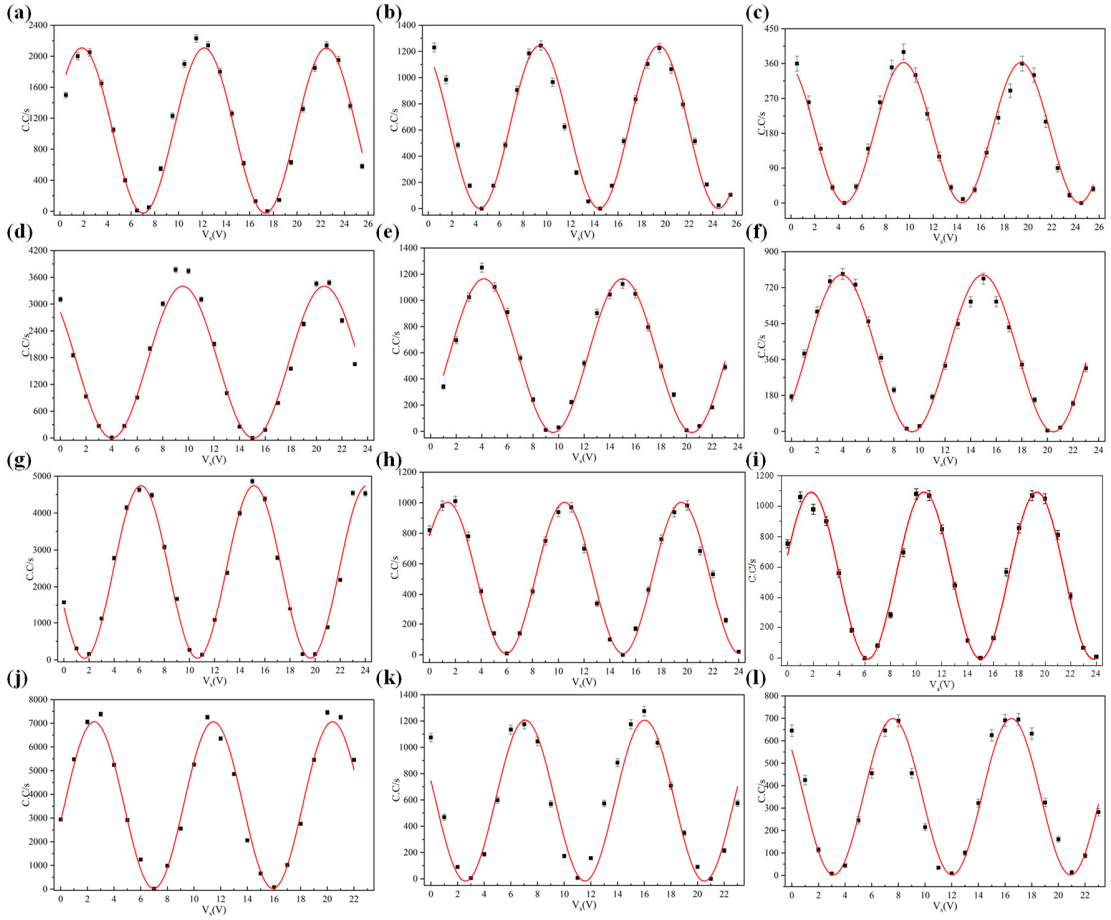

Fig.S2 BRHOM interference of degenerate and nondegenerate photon pairs. (a)-(c) The $|1,1\rangle$, $|2,0\rangle$ and $|0,2\rangle$ of 1523.6 nm photon pairs vary with the V_c. (d)- (f) The $|1,1\rangle$, $|2,0\rangle$ and $|0,2\rangle$ of 1601 nm photon pairs vary with the V_c. (g)- (i) The $|1,1\rangle$, $|2,0\rangle$ and $|0,2\rangle$ of photon pairs with a separation of 20 nm vary with the V_c. (j)- (i) The $|1,1\rangle$, $|2,0\rangle$ and $|0,2\rangle$ of photon pairs with a separation of 60 nm vary with the V_c. Error bars show $\sqrt{\pm\text{counts}}$.

Note 4: off-chip HOM interference for degenerate and nondegenerate photons

The main text has given examples of HOM interference for a pair of photons with 1565 nm and with a separation of 40 nm. In this part, we will give the remaining interference fringes.

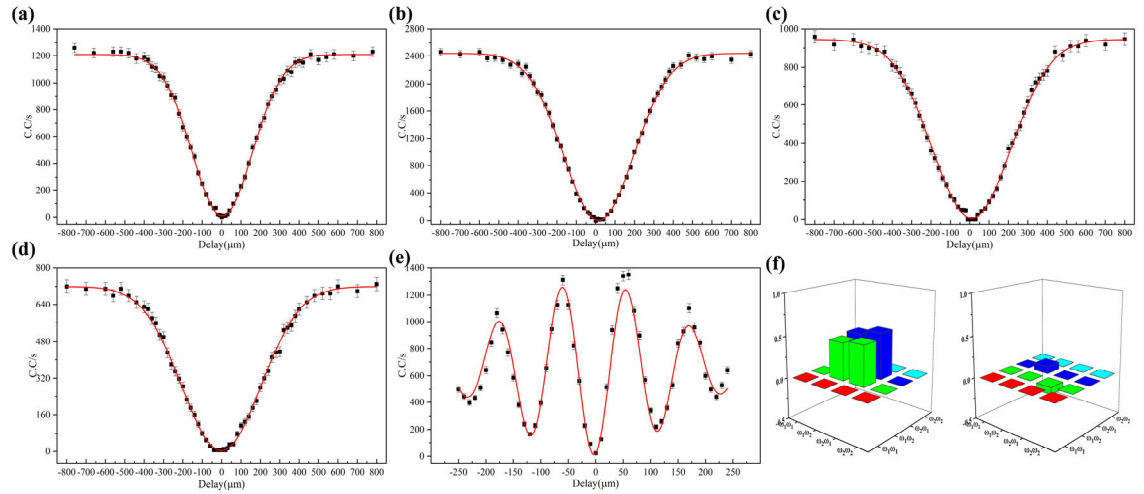

Fig.S3 HOM interference of degenerate and nondegenerate photon pairs. (a)-(d) HOM interference for identical photon pairs with 1523.6 nm, 1542 nm, 1582 nm and 1601 nm, respectively. (e) The HOM interference for frequency entangled photon pairs with a separation of 20 nm. (f) Reconstructed density matrix based on the fringes in Fig. 2(e). Error bars show $\sqrt{\pm \text{counts}}$.

The results exhibit that our source not only has high quality, but also has considerable brightness.

Note 5: Fidelity estimation of path entanglement

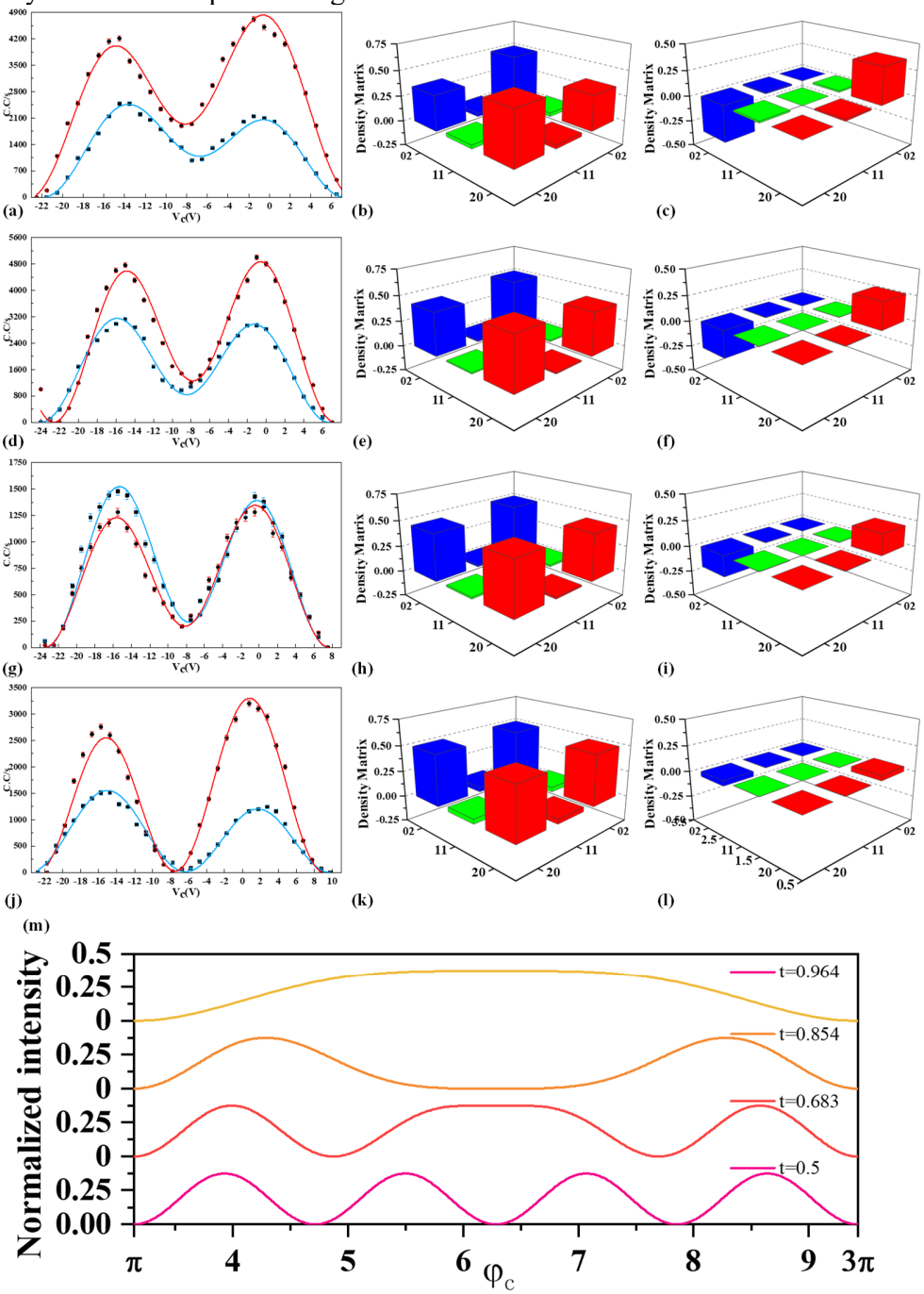

Fig.S4 (a), (d), (g) and (j) The measured $|0,2\rangle_p$ (red square dots), $|2,0\rangle_p$ (blue round dots) coincidence counts and $|0,2\rangle_p$ (red), $|2,0\rangle_p$ (blue) fitting curves of 1582 nm, 1565 nm, 1542nm and 1523.6 nm photon pairs, respectively. (b), (e), (h) and (k) the real part of estimated density matrix for corresponding photons. (c), (f), (i) and (l) the imaginary part of estimated density matrix for corresponding photons. (m) Theoretical 'phase-resolution reduced' interference of input state $|2,2\rangle$. Error bars show $\sqrt{\pm\text{counts}}$.

Table S1. The $t_{|2,0\rangle}$, $t_{|0,2\rangle}$, $m_{|2,0\rangle}$ and $m_{|0,2\rangle}$ come from fitting of each curve. The *t* is picked from Fig. 2(d) according to the wavelength. Error bars show $\sqrt{\pm\text{counts}}$. The results are summarized in followed table.

Wavelengh	$t_{\|2,0\rangle}$	$t_{\|0,2\rangle}$	t_g	t	$m_{\|2,0\rangle}$	$m_{\|0,2\rangle}$	m
1523.6 nm	0.539 ± 0.005	0.520 ± 0.015	0.525±0.010	0.500	0.914 ± 0.013	0.893 ± 0.012	0.8794± 0.0101
1542 nm	0.607 ± 0.007	0.606 ± 0.007	0.602±0.005	0.560	0.926 ± 0.018	0.974 ± 0.014	0.9536± 0.0137
1565 nm	0.645 ± 0.004	0.627 ± 0.007	0.635±0.004	0.642	0.985 ± 0.013	0.957 ± 0.017	0.9685± 0.0117
1582 nm	0.683 ± 0.004	0.687 ± 0.007	0.683±0.004	0.702	0.936 ± 0.013	0.880 ± 0.017	0.8973± 0.0121
1601 nm	0.717 ± 0.003	0.711 ± 0.002	0.716±0.003	0.745	0.905 ± 0.016	0.936 ± 0.011	0.9201± 0.0087

Sensitive probe state can estimate the parameters. We fix $\varphi_s = 2\,\mathrm{Re}(A_0)$ and observe the variation of $|2,0\rangle_p$ and $|0,2\rangle_p$ with φ_c for different wavelength photons. Measurements are shown in Fig. S3 (a), (d), (g) and (j). Least squares method provides the estimations of *m* and *t* from the data. Through global fitting, (m and *t* are set as shared parameters), we can obtain more precise and reasonable estimates shown in Tab. S1. Then, the estimated real and imaginary part of density matrices are plotted in Fig S4 (b), (e), (h), (k) and (c), (f), (i), (l), respectively.

$t_{|2,0\rangle}$, $t_{|0,2\rangle}$ and t_g are close to the *t*, which represents the method that measuring tested components is credible. $m_{|2,0\rangle}$ and $m_{|0,2\rangle}$ are close to each other. Based on Eq. S(14) and Tab. S1, the measured visibilities of HOM interference in Tab. 2 are compatible with theoretical values.

Fig. S4 (m) is the theoretical 'phase-resolution reduced' interference of input state $|2,2\rangle$. Observation of $|3,1\rangle$ shows that the oscillation frequencies degrade from four to one in 2π phase range, which make pattern more sensitive than two photon interference.

Note 6: Beating the Standard Quantum Limit with our resources

It is well known that the NOON state can apply in quantum optical metrology [1, 2]. The *phase super-resolution* [3] is easy to be observed, while *phase super-sensitivity* is not [4, 5]. The quality of quantum state limits the ability to beat the Standard Quantum Limit (SQL) of *phase super-sensitivity*.

Our resources have an advantage in quality and can be quantified by parameter *m* according to Supplementary Note 1. In the previous works [4, 5], $|2,2\rangle$ is the input state and $|3,1\rangle$ is observed state. The down-converted light is filtered for uncorrelated photons [6]. Based the Eq. (14), the normalized 4-photons output expression is

$$|\psi\rangle_{4\text{-p}}=\frac{1+m^2}{\sqrt{6+4m^2+6m^4}}\left(\frac{\left(\hat{\mathrm{R}}_1^{\dagger}\right)^2 \mathrm{e}^{-\frac{\mathrm{i}\varphi_s}{2}}\left(-1+\mathrm{e}^{\mathrm{i}\varphi_s}m\right)}{2\sqrt{2}\sqrt{1+m^2}}-\frac{\left(\hat{\mathrm{R}}_2^{\dagger}\right)^2 \mathrm{e}^{-\frac{\mathrm{i}\varphi_s}{2}}\left(-1+\mathrm{e}^{\mathrm{i}\varphi_s}m\right)}{2\sqrt{2}\sqrt{1+m^2}}+\frac{\mathrm{i}\hat{\mathrm{R}}_1^{\dagger}\hat{\mathrm{R}}_2^{\dagger}\mathrm{e}^{-\frac{\mathrm{i}\varphi_s}{2}}\left(1+\mathrm{e}^{\mathrm{i}\varphi_s}m\right)}{\sqrt{2}\sqrt{1+m^2}}\right)^2. \tag{15}$$

If $\varphi_{\mathrm{s}}=0$, the output state is mostly composed of $|2,2\rangle$. After evolving on another $\mathrm{MZI_{QM}}$ used in quantum metrology, $|\psi\rangle_{4\text{-p}}(\varphi_{\mathrm{s}}=0)\rightarrow|\psi'\rangle_{4\text{-p}}$, the relationship between the $|3,1\rangle$ and phase (φ) in $\mathrm{MZI_{QM}}$ is

$$P_{|3,1\rangle}=\left|\langle 3,1|\psi'\rangle_{4\text{-p}}\right|^2=\left|\frac{\mathrm{i}\left(\mathrm{e}^{4\mathrm{i}\varphi}-m^2\right)}{2\sqrt{6+4m^2+6m^4}}\right|^2=\frac{3\left(1+m^4-2m^2\cos\left(4\varphi\right)\right)}{4\left(3+2m^2+3m^4\right)}. \tag{16}$$

Referring the works [74, 76], the SQL of 4-photons Fisher information (FI) is 4. The Fisher information of our resources is

$$\mathrm{FI}_{|3,1\rangle}=\frac{192m^4\cos\left(4x_0\right)^2}{\left(9+8m^2+9m^4-6m^2\sin\left(4x_0\right)\right)\left(1+m^4+2m^2\sin\left(4x_0\right)\right)}. \tag{17}$$

where x_0 is bias phase. Only when *m* is large enough and x_0 is in a specific interval can FI beat the SQL, as shown in Fig. S5. The maximum of FI can figure out by

$$\mathrm{Max}_{\mathrm{FI}}=\frac{16}{2\left(3+4m^2+3m^4\right)^2}. \tag{18}$$
$$1+\frac{}{3\left(9+8m^2+6m^4+8m^6+9m^8-\left(1-m^4\right)\sqrt{81+144m^2+190m^4+144m^6+81m^8}\right)}$$

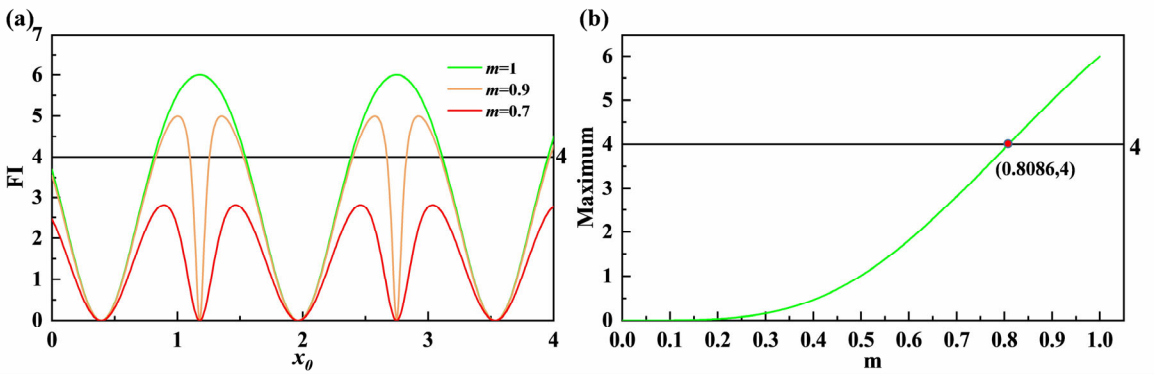

Fig.S5 The Fisher information of $|3,1\rangle$. (a) The FI varies with x_0 at different *m*. (b) The maximum of FI varies with the *m*.

The threshold of *m* that can beat SQL is 0.8086, corresponding to 97.78% visibility of HOM (BRHOM) interference. Based on the measurement in Tab. S1, our resources can qualify the quantum metrology.

References

[1]. J. P. Dowling, "Quantum optical metrology – the lowdown on high-N00N states," Contemp. Phys. **49**, 125–143 (2008)

[2]. E. Polino, M. Valeri, N. Spagnolo, and F. Sciarrino, "Photonic quantum metrology," AVS Quantum Sci. **2**, 024703 (2020).

[3]. M. W. Mitchell, J. S. Lundeen, and A. M. Steinberg, "Super-resolving phase measurements with a multiphoton entangled state," Nature **429**, 161-164 (2004).

[4]. T. Nagata, R. Okamoto, J. L. O'Brien, K. Sasaki, and S. Takeuchi, "Beating the standard quantum limit with four-entangled photons," Science **316**, 726-729 (2007).

[5]. R. Okamoto, H. F Hofmann, T. Nagata, J. L O'Brien, K. Sasaki, and S. Takeuchi, "Beating the standard quantum limit: phase super-sensitivity of N-photon interferometers," New J. Phys. **10**, 073033 (2008).

[6]. Bao, J., Fu, Z., Pramanik, T. et al. "Very-large-scale integrated quantum graph photonics," Nat. Photon. **17**, 573–581 (2023).